

# Investigation of the properties of metal oxide compounds in superconducting and normal states

N. E. Alekseevskii, E. P. Khlybov, G. M. Kuz'micheva, V. V. Evdokimova, A. V. Mitin, V. K. Nizhankovskii, and A. I. Kar'kovskii

*S. I. Vavilov Institute of Physics Problems, Academy of Sciences of the USSR, Moscow*

(Submitted 29 September 1987)

Zh. Eksp. Teor. Fiz. **94**, 281–294 (May 1988)

An x-ray phase analysis was made of superconducting compounds in the RE–Ba–Cu–O system, where RE is yttrium and the whole rare-element series with the exception of promethium. A study was made of the relationship between the critical temperature  $T_c$  of the superconducting transition, on the one hand, and the parameters of the unit cell and the phase composition of the samples, on the other. Electrophysical and magnetic properties were determined in a wide range of magnetic fields (up to 500 kOe) and temperatures. An analysis of the experimental data [such as the correlation of  $T_c$  with the orthorhombic distortion of the crystal structure, a weak influence of the magnetic moment of the RE element on  $T_c$ , high values of the second critical field  $H_{c2}(T)$ , and a linear temperature dependence of the resistance in the range  $T > T_c$ ] demonstrated the importance of copper-oxygen chains in the formation of the superconducting state in REBa<sub>2</sub>Cu<sub>3</sub>O<sub>7-x</sub> compounds.

The discovery, by Bednorz and Müller,<sup>1</sup> of the  $T_c \approx 30$  K superconductivity in the La–Ba–Cu–O system has stimulated the search for new high-temperature superconductors among metal oxides containing rare-earth elements. Already in March 1987 Chu *et al.*<sup>2</sup> reported observation of a superconducting transition in the Y–Ba–Cu–O system at a temperature of about 90 K. Quite quickly these results were reproduced in many laboratories around the world.

The present paper reports synthesis of high-temperature superconductors in the Y–Ba–Cu–O and RE–Ba–Cu–O systems, where RE is the whole series of rare earths with the exception of promethium. We shall describe a detailed investigation of the relationship between  $T_c$  of these superconductors, on the one hand, and the unit cell parameters and the phase composition of the samples, on the other. We shall report the results of measurements of electrical and magnetic properties of samples belonging to these systems, in the superconducting and normal states, carried out in a wide range of magnetic fields and temperatures.

## 1. INFLUENCE OF THE STRUCTURE CHARACTERISTICS ON $T_c$

Our samples were prepared mainly by the method of reaction in the solid phase.<sup>3</sup> The initial components were rare-earth oxides (BaCO<sub>3</sub>, BaO, or BaO<sub>2</sub>) and also copper oxide. Powders of the components were taken in the appropriate proportions, mixed carefully, and sintered at 900–1050 °C for 6–10 h in air or in an oxygen atmosphere. Before a homogenizing annealing the samples were ground again and compacted into pellets. The annealing took place at 800–1050 °C and it lasted 10 h. If necessary, the whole procedure was repeated many times. In some cases the original mixture of powders used in the synthesis was produced by coprecipitation of nitrates with the aid of oxalic acid.<sup>1</sup>

An x-ray phase analysis was carried out by comparing the powder diffractograms (recorded using a DRON-2.0 unit, Cu  $K_\alpha$  radiation, and a graphite monochromator) with the ASTM file data and also with the results given in Ref. 4. The unit cell parameters were calculated from the diffrac-

tion reflections in the angular range  $2\theta = 75\text{--}105^\circ$  for the phase of the REBa<sub>2</sub>Cu<sub>3</sub>O<sub>7-x</sub> (1–2–3) structure type and in the range  $2\theta = 30\text{--}72^\circ$  for the K<sub>2</sub>NiF<sub>4</sub> (2–1–4) structure type.

An x-ray phase analysis showed that synthesis of samples with compositions described by (RE, Ba)<sub>2</sub>CuO<sub>4-x</sub> produced a mixture of phases of the 1–2–3 and 2–1–4 structure types and a phase with the composition RE<sub>2</sub>CuO<sub>5</sub>. The use of charges with the composition REBa<sub>2</sub>Cu<sub>3</sub>O<sub>7-x</sub> yielded both single-phase and multiphase samples in which the impurities were in the form of RE<sub>2</sub>BaCuO<sub>5</sub> or CuO, and less frequently BaCO<sub>3</sub> or RE<sub>2</sub>Cu<sub>2</sub>O<sub>5</sub>. The presence of extraneous phases was typical of samples which were compounds of Pr, Tb, Yb, and Lu. Sometimes the impurity was in the form of a phase of the K<sub>2</sub>NiF<sub>4</sub> type. For example, such a phase was observed for some samples with the 1–2–3 composition containing Y, Ho, Er, Tm, Yb, and Lu. It should be pointed out that the appearance of a phase with the K<sub>2</sub>NiF<sub>4</sub> structure type was deduced from the superconducting transition curves measured by an inductive method, because these curves exhibited not only a superconducting transition at  $T_c \approx 90$  K, but also a second transition at  $T_c \approx 40$  K. This result could indicate that the investigated class of high-temperature superconductors contained two superconducting phases: one with the 1–2–3 structure and  $T_c \approx 90$  K and the other with the 2–1–4 structure and  $T_c \approx 40$  K.

Table I gives the unit cell parameters of the 1–2–3 phase, the temperatures at the onset of the superconducting transition  $T_c$ , and the width of the transition  $\Delta T_c$  measured by an inductive method between the values representing 0.1–0.9 of the maximum. It should be pointed out that the superconducting transition curves deduced from the resistance were usually much narrower and coincided with the onset of the inductive transition. Table II gives the cell parameters for phases of the 2–1–4 structure type.

Usually the unit cell parameters of isostructural compounds containing rare-earth elements decrease on increase in the atomic number of the RE element because of a reduction of the ionic radius (lanthanoid compression). However,

TABLE I. Results of x-ray diffraction investigations of phases in REBa<sub>2</sub>Cu<sub>3</sub>O<sub>7-x</sub> samples.

RE	Cell parameters, Å			T <sub>c</sub> , K	ΔT <sub>o</sub> , K
	a±0,002	b±0,001	c±0,005		
La	3.912	3.912	11.738	Non-superconducting	
La	3.90(1)	3.92(1)	11.73(2)	71	30
Ce	3.89	3.91	11.73	86	16
Pr	3.889	3.904	11.691	69	35
Nd	3.880	3.900	11.690	55	30
Nd	3.828	3.870	11.680	83	18
Sm	3.852	3.890	11.685	84	18
Eu	3.855	3.882	11.690	75	24
Eu	3.828	3.879	11.660	96	12
Eu	3.834	3.876	11.660	89	15
Gd	3.843	3.882	11.680	88	9
Gd	3.848	3.882	11.680	84	12
Tb	3.830	3.872	11.632	89	6
Dy	3.835	3.878	11.650	87	9
Y	3.842	3.874	11.642	64	25
Y	3.823	3.875	11.642	91	9
Y	3.840	3.887	11.676	79	26
Y	3.828	3.875	11.675	89	12
Y	3.812	3.874	11.635	94	5
Ho	3.834	3.876	11.633	90	6
Er	3.834	3.876	11.660	88	20
Er	3.828	3.876	11.638	95	3
Tm	3.840	3.874	11.685	89	7
Yb	3.854	3.874	11.563	89	6
Lu	3.844	3.873	11.605	89	5
Lu	3.854	3.870	11.574	88	15

it follows from the results in Table I that such a dependence was not monotonic in the case of the investigated high-temperature superconductors. Moreover, in the case of different samples of the same charge composition the unit cell parameters could differ considerably, depending on the conditions during preparation. This could be due to deviation of the compositions of the samples from stoichiometry, particularly due to different concentrations of oxygen. One could not exclude the possibility of a change in the valence state of a rare-earth metal and copper.

It should be stressed that our results provided clear evidence of a correlation between T<sub>c</sub> and the orthorhombic distortion of the unit cell (b - a)/(b + a). This distortion was related to the concentration of oxygen in the samples. For example, samples with a lower oxygen content prepared by annealing in vacuum, as well as samples quenched from high temperatures did not exhibit the orthorhombic distortion and did not go over to the superconducting state. Under optimal annealing conditions the orthorhombic distortion became maximal and the value of T<sub>c</sub> reached 95 K irrespective of the nature of the rare-earth metal. A further increase in the amount of oxygen (achieved by increasing its pressure during annealing) reduced the orthorhombic distortion and

the value of T<sub>c</sub> until the superconductivity disappeared completely.

Figure 1 shows the changes in T<sub>c</sub> observed for YBa<sub>2</sub>Cu<sub>3</sub>O<sub>7-x</sub> samples as a function of the orthorhombic distortion (b - a)/(b + a). Similar dependences were obtained by us for compounds of all the other rare-earth elements. An additional increase in the "splitting" between the parameters a and b resulted when a fraction of an oxide in the initial charge was replaced with a fluoride. The superconducting transition temperature then increased to 104 K, but such samples were unstable and after several days their superconducting transition temperature T<sub>c</sub> fell to 92-94 K.

The correlation between T<sub>c</sub> and the orthorhombic distortion of the unit cell can be understood by considering the structure of compounds of the REBa<sub>2</sub>Cu<sub>3</sub>O<sub>7-x</sub> type (Ref. 4), as demonstrated in Fig. 2. In this structure an oxygen ion can occupy five different positions, but oxygen vacancies can form only in the planes containing Cu1. When the concentration of oxygen is optimal (x ≈ 0), the oxygen ions occupy preferentially the positions such that one-dimensional -O-Cu1-O- chains form along the b direction in the basal plane. The orthorhombic distortion is then maximal. Reduction in the oxygen content breaks up the -O-Cu1-O-chains

TABLE II. Results of x-ray diffraction investigations of phases of the K<sub>2</sub>NiF<sub>4</sub> type in samples with the initial charge composition (RE, Ba)<sub>2</sub>CuO<sub>4-x</sub>.

	Composition of initial charge	Cell parameters, Å	
		a±0,005	c±0,02
1	(Y <sub>0,6</sub> Ba <sub>0,4</sub> ) <sub>1,8</sub> CuO <sub>4-x</sub>	3.775	13.54
2	(Y <sub>0,6</sub> Ba <sub>0,4</sub> ) <sub>2</sub> CuO <sub>4-x</sub>	3.790	13.54
3	(Y <sub>0,5</sub> Th <sub>0,1</sub> Ba <sub>0,4</sub> ) <sub>1,8</sub> CuO <sub>4-x</sub>	3.812	13.64
4	(Ho <sub>0,6</sub> Ba <sub>0,4</sub> ) <sub>2</sub> CuO <sub>4-x</sub>	3.799	13.46
5	(Er <sub>0,55</sub> Ba <sub>0,45</sub> ) <sub>2</sub> CuO <sub>4-x</sub>	3.780	13.35
6	(Er <sub>0,4</sub> Ba <sub>0,6</sub> ) <sub>2</sub> CuO <sub>4-x</sub>	3.811	13.53
7	(Tm <sub>0,62</sub> Ba <sub>0,38</sub> ) <sub>2</sub> CuO <sub>4-x</sub>	3.771	13.36
8	(Yb <sub>0,58</sub> Ba <sub>0,42</sub> ) <sub>2</sub> CuO <sub>4-x</sub>	3.745	13.32

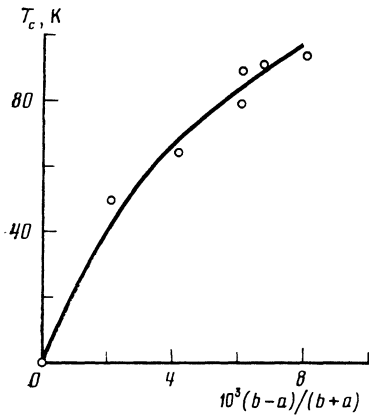


FIG. 1. Influence of the orthorhombic distortion on the temperature  $T_c$  of  $\text{YBa}_2\text{Cu}_3\text{O}_{7-x}$  samples.

and causes localization of the carriers. A consequence is a reduction in the conductivity  $\sigma$  and a fall of  $T_c$ . The orthorhombic distortion then decreases.

On the other hand, the orthorhombic distortion decreases also on increase in the oxygen content above the optimal value, because this results in filling of the remaining oxygen vacancies along the direction  $a$  and the crystal structure becomes more symmetric. A two-dimensional network is formed instead of  $-\text{O}-\text{Cu}1-\text{O}-$  chains in the basal plane.

## 2. MAGNETIC PROPERTIES

Magnetic properties were investigated by a variety of methods using a fluxmeter, a string magnetometer, a Faraday balance, a weak alternating magnetic field (inductive method for the determination of the critical temperatures), and an hf magnetometer with a SQUID as a null indicator. Figure 3 shows the temperature dependences of the magnetic susceptibility  $\chi$  of Y-Ba-Cu-O samples with different initial compositions of the charge, determined in the normal state (these measurements were made using a Faraday balance in a field of 3.1 kOe). It is clear from Fig. 3 that the sample with the 1-2-3 composition and closest to the single phase had the lowest magnetic susceptibility, which varied little with temperature. The susceptibility of the other two

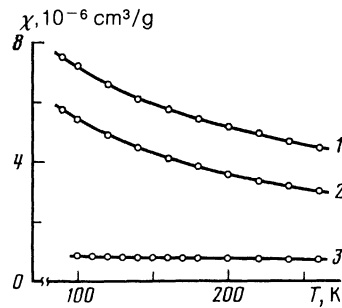


FIG. 3. Temperature dependences of the magnetic susceptibility: 1)  $\text{Y}_{1.08}\text{Ba}_{0.72}\text{CuO}_{4-x}$ ; 2)  $\text{Y}_{1.2}\text{Ba}_{0.8}\text{CuO}_{4-x}$ ; 3)  $\text{YBa}_2\text{Cu}_3\text{O}_{7-x}$ .

samples fitted well the usual dependence

$$\chi = \chi_0 + N_A \mu_{\text{eff}}^2 / 3k_B M (T - \Theta), \quad (1)$$

where  $N_A$  is the Avogadro number;  $M$  is the molecular weight,  $k_B$  is the Boltzmann constant;  $\Theta$  is the Curie temperature.

The effective magnetic moment per formula unit  $\mu_{\text{eff}} = (1.5-2.0)\mu_B$  indicated the presence of the  $\text{Cu}^{2+}$  ions in these samples. This result was confirmed by preliminary ESR data. The temperature-independent component  $\chi_0 = (0.6-0.8) \times 10^{-6} \text{ cm}^3/\text{g}$  was close to the magnetic susceptibility of a sample with the 1-2-3 composition. Assuming that  $\chi_0$  was due to the Pauli spin paramagnetism, we estimated the electron specific heat to be  $\gamma \approx 40 \text{ mJ} \cdot \text{mol}^{-1} \cdot \text{K}^{-2}$ .

The  $\chi^{-1}(T)$  dependences obtained for the samples containing rare-earth elements with localized magnetic moments (Fig. 4) obeyed the Curie-Weiss law and the values of  $\mu_{\text{eff}}$  were close to those calculated on the assumption of the presence of free  $\text{RE}^{3+}$  ions (Table III) and the negative sign of the Curie temperature  $\Theta$  indicated the possibility of antiferromagnetic ordering. Such ordering was indeed observed for  $\text{GdBa}_2\text{Cu}_3\text{O}_{7-x}$  (Ref. 5).

Figure 5 shows the field dependence of the magnetic moment of a sample of  $\text{GdBa}_2\text{Cu}_3\text{O}_{7-x}$  measured using a string magnetometer at  $T = 4.2 \text{ K}$ . In fields below 6 kOe the magnetic moment was negative, as expected for conventional superconductors. In fields exceeding 6 kOe the magnetic moment became positive and tended to saturation in stronger magnetic fields. The sample remained in the supercon-

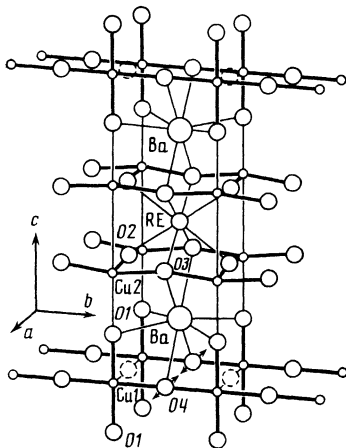


FIG. 2. Structure of compounds of the  $\text{REBa}_2\text{Cu}_3\text{O}_{7-x}$  type.<sup>4</sup>

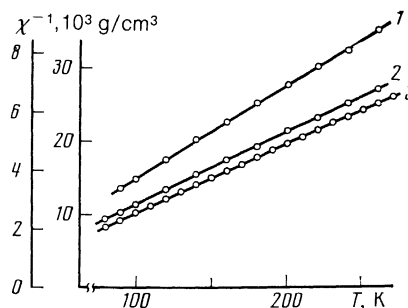


FIG. 4. Dependences of the reciprocal of the magnetic susceptibility on the temperature of RE-Ba-Cu-O samples containing rare-earth magnetic elements: 1) RE = Er; 2) RE = Ho; 3) RE = Gd (inner scale).

TABLE III. Magnetic properties of samples containing rare earths with localized magnetic moments (the effective moment is given per rare-earth ion).

Composition	$\mu_{\text{eff}}, \mu_B$	$\theta, \text{K}$	$\mu_{\text{RE}^{3+}}, \mu_B$
NdBa <sub>2</sub> Cu <sub>3</sub> O <sub>7-x</sub>	3.5	-20	3.6
GdBa <sub>2</sub> Cu <sub>3</sub> O <sub>7-x</sub>	7.8	-5	7.9
Ho <sub>1.2</sub> Ba <sub>0.8</sub> CuO <sub>4-x</sub>	9.9	-14	10.6
Er <sub>1.2</sub> Ba <sub>0.8</sub> CuO <sub>4-x</sub>	8.7	-14	9.6
Yb <sub>0.98</sub> Ba <sub>0.72</sub> CuO <sub>4-x</sub>	4.3	-40	4.5

ducting state, as demonstrated by hysteresis of the magnetic moment. The average dependence of the magnetic moment on the field could be described satisfactorily by the Brillouin function with  $J = 7/2$  corresponding to the total moment of the Gd<sup>3+</sup> ion (dashed curve in Fig. 5) and the relatively small deviation could be associated with the proximity of the temperature during experiments to the antiferromagnetic ordering point  $T_N = 2.2 \text{ K}$  (Ref. 5).

The screening of the magnetic field was studied using a magnetometer with a SQUID in the following sequence. First, a sample was cooled in the absence of a magnetic field to  $T = 4.2 \text{ K}$ . Then, a solenoid operating in the nondecaying current regime created the required magnetic field. The magnetic moment measurements were made while the temperature was increasing from 4.2 K to  $T_c$ . The results of the measurements (Figs. 6 and 7) indicated that even in weak magnetic fields the magnetic moment measured at temperatures  $T \ll T_c$  was more than twice the value expected in the case of ideal diamagnetism. This difference could be due to not only the presence of additional phases in the samples, but also due to the fine-grain structure of the sample when the characteristic grain size was only slightly greater than the depth of penetration of the field  $\lambda$ . This hypothesis was confirmed by the dependence of the magnetic moment on the external magnetic field measured in the superconducting state at various temperatures (Fig. 8). Such dependences were typical of type II superconductors: the magnetic moment varied linearly in fields below  $H_{c1}$  and this was followed by a maximum and a smooth fall of the moment as a result of cooling. This effect increased the magnetic susceptibility  $\chi = -(\partial M / \partial H)_{H \rightarrow 0}$  from  $6 \times 10^{-3}$  at  $T = 40 \text{ K}$  to  $25 \times 10^{-3}$  at  $T = 4.2 \text{ K}$ , which represented  $\sim 30\%$  of the value corresponding to ideal diamagnetism (after correction for the paramagnetic susceptibility of the Gd<sup>3+</sup> ions). A similar behavior of  $\chi$  had been reported, for example, for colloidal mercury<sup>6</sup> and could be explained satisfactorily by

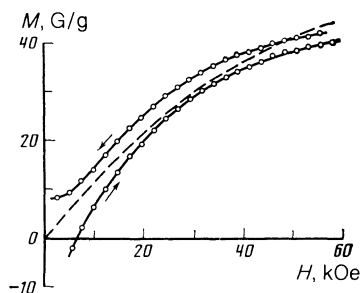


FIG. 5. Dependence of the magnetic moment of GdBa<sub>2</sub>Cu<sub>3</sub>O<sub>7-x</sub> on the magnetic field.

the temperature dependence of the penetration depth  $\lambda$ . These ideas and results of electron-microscopic examinations made it possible to estimate the depth of penetration, which was  $\lambda(0) \approx 0.1-0.5 \mu\text{m}$  for GdBa<sub>2</sub>Cu<sub>3</sub>O<sub>7-x</sub>.

### 3. CRITICAL MAGNETIC FIELDS

The first critical magnetic field  $H_{c1}$  was deduced from the linear parts of the reversible magnetization curves  $M(H)$  shown in Fig. 8. The temperature dependences  $H_{c1}(T)$  obtained for samples containing Y, Lu, and Gd were plotted allowing for the demagnetization factor (Fig. 9). The results obtained indicated that the presence of the RE<sup>3+</sup> ions with localized magnetic moments (for example, Gd<sup>3+</sup> in the crystal structure of a superconductor had no significant influence on the value of  $H_{c1}(T)$  at low temperatures.

Since electron micrographs demonstrated that the investigated samples consisted of randomly oriented grains (crystallites), the properties of which could be anisotropic, it was reasonable to assume that the values  $H_{c1}(T)$  plotted in Fig. 9 were governed mainly by the direction along which  $H_{c1}(T)$  was minimal. This was supported in particular by a comparison of the value of  $H_{c1}(4.2 \text{ K}) \approx 600 \text{ Oe}$  for a polycrystalline sample containing Y (Fig. 9) with the recently published<sup>7</sup> values of  $H_{c1}^{\parallel}(4.5 \text{ K}) = 530-800 \text{ Oe}$  and  $H_{c1}^{\perp}(4.5 \text{ K}) = 5.2-8 \text{ kOe}$  obtained for a YBa<sub>2</sub>Cu<sub>3</sub>O<sub>7-x</sub> single crystal oriented relative to the basal plane.

The second critical field was found from the resistive curves  $H_{c2}$  of the superconducting transition  $\rho(T, H)$  obtained using static (up to 100 kOe) and pulsed (up to 500 kOe) magnetic fields. In the latter case we used the apparatus employed earlier to determine the  $H_{c2}(T)$  dependence for molybdenum chalcogenides.<sup>8</sup> When measurements were

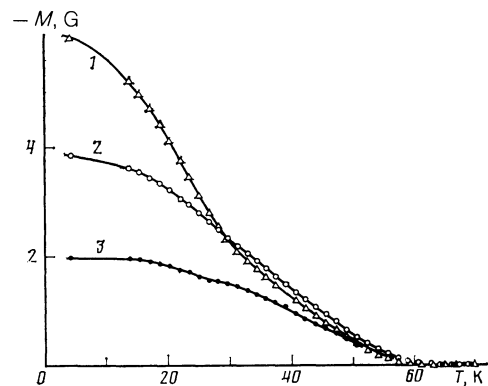


FIG. 6. Temperature dependences of the magnetic moment of GdBa<sub>2</sub>Cu<sub>3</sub>O<sub>7-x</sub> measured in static fields  $H$ : 1)  $H = 500 \text{ Oe}$ ; 2)  $H = 250 \text{ Oe}$ ; 3)  $H = 75 \text{ Oe}$ .

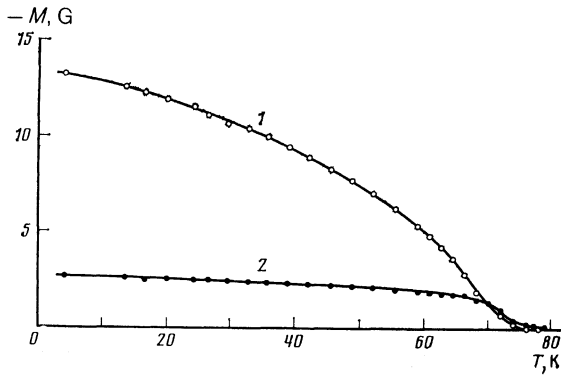


FIG. 7. Temperature dependences of the magnetic moment of  $Y_{1.08}Ba_{0.72}CuO_{4-x}$  measured in static fields  $H$ : 1) 500 Oe; 2) 50 Oe.

made in pulsed magnetic fields, the transition curves were plotted on the basis of a change in the voltage across potential contacts through which an alternating current of frequency 2–10 kHz and  $\sim 10$  mA amplitude was passed. Samples of 4–8 mm length and of  $0.5\text{--}1$  mm<sup>2</sup> cross section were mounted in a holder at right-angles to the magnetic field. The holder ensured reliable thermal contact with liquid or gaseous nitrogen. Possible heating in a varying magnetic field<sup>9</sup> was avoided by plotting the transition curves on the basis of only those values of the signal which corresponded to the maximum amplitudes of the field.

It had been reported in many papers<sup>2,5</sup> that an increase in the field caused strong broadening of the lower parts of the superconducting transition curves (i.e., in the range  $\rho < 0.5\rho_n$ ). A comparison of the results obtained for samples of similar compositions showed that the relative magnitude of such broadening was largely governed by the microstructure of the samples, which in turn depended on the conditions during preparation. We could therefore conclude that the anomalous broadening of the  $\rho(T, H)$  curves at low values of  $\rho$  was due to an inhomogeneity of the sample primarily near the grain boundaries where even weak fields  $H \ll H_{c2}$  were sufficient to suppress the superconductivity. Such

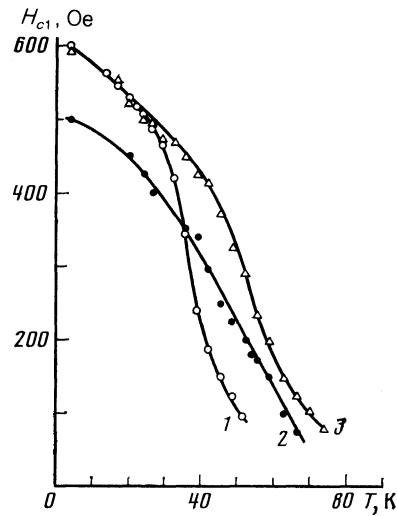


FIG. 9. Temperature dependences of the first critical magnetic field of RE-Ba-Cu-O samples.: 1) RE = Gd; 2) RE = Lu; 3) RE = Y.

broadening was particularly strong at low values of the coherence length  $\xi$ .

The steepest superconducting transition curves were observed in a magnetic field for compact samples in which the binding of the grains was strong, as indicated by a fairly high density of the critical current  $J_c$  (77 K)  $> 100$  A/cm<sup>2</sup>. Nevertheless, even in the case of these samples the magnetic field broadened considerably the transition curves (Figs. 10 and 11) and this could be due to an inhomogeneity or an anisotropy of  $H_{c2}$ .

The value of  $H_{c2}$  was taken to be the field corresponding to the middle of the superconducting transition curve ( $0.5\rho_n$ ). We used this criterion to plot the  $H_{c2}(T)$  dependences shown in Fig. 12 for samples with Y and Lu. The maximum values of the derivatives  $|\partial H_{c2}/\partial T|_{\max}$  for samples with Y and Lu were then 25 and 20 kOe/K, respectively. However, if the critical field was determined from the onset

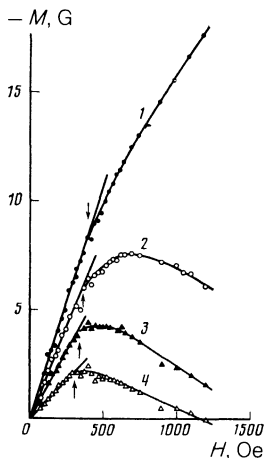


FIG. 8. Magnetization curves of  $GdBa_2Cu_3O_{7-x}$  in the superconducting state: 1)  $T = 4.2$  K; 2)  $T = 17.0$  K; 3)  $T = 24.4$  K; 4)  $T = 29.6$  K. The arrows identify the fields corresponding to  $H_{c1}$ .

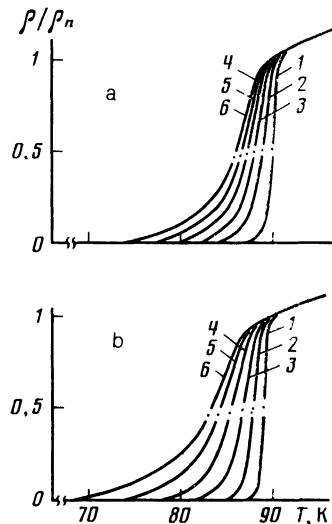


FIG. 10. Superconducting transition curves of Y-Ba-Cu-O (a) and Lu-Ba-Cu-O (b) samples determined in static magnetic fields  $H$  (kOe): 1) 0; 2) 10; 3) 20; 4) 40; 5) 60; 6) 80.

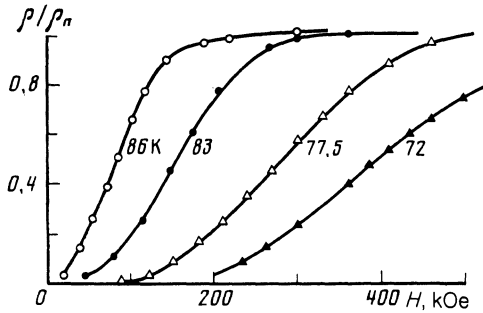


FIG. 11. Superconducting transition temperatures of Y-Ba-Cu-O samples recorded in pulsed magnetic fields at fixed temperatures.

of the superconducting transition, the  $H_{c2}^*(T)$  dependences were much steeper and the derivatives were  $|\partial H_{c2}^*/\partial T|_{\max} = 50$  and  $40$  kOe/K for samples with Y and Lu, respectively.

We estimated  $H_{c2}(0)$  from the relationship

$$H_{c2}(0) \approx 0.7T_c |\partial H_{c2}/\partial T|_{\max},$$

which was satisfied reasonably well by, for example, molybdenum sulfides<sup>8</sup> with approximately the same values of  $|\partial H_{c2}^*/\partial T|_{\max}$ . In the case of the sample with Y we found that  $H_{c2}(0) \approx 1.5$  MOe and  $H_{c2}^*(0) \approx 3$  MOe.

We could estimate the values of  $H_{c2}(0)$  and  $H_{c2}^*(0)$  also from the experimental data for  $H_{c1}(T)$ . Using the relationships<sup>10</sup>

$$\begin{aligned} H_{c1}(T) &= \frac{H_c(T)}{2^{1/2}\kappa_3(T)} \ln \kappa_3(T), \\ H_{c2}(T) &= 2^{1/2}\kappa_1(T) H_c(T), \end{aligned} \quad (2)$$

and bearing in mind that  $\kappa_1 = \kappa_3 = \kappa$  in the limit  $T \rightarrow T_c$ , we found that

$$\left. \frac{\partial H_{c2}}{\partial T} \right|_{T \rightarrow T_c} = \frac{2\kappa^2}{\ln \kappa} \left. \frac{\partial H_{c1}}{\partial T} \right|_{T \rightarrow T_c} \quad (3)$$

Using the experimental values for the sample with Y we obtained  $\kappa = 60$  and  $\kappa^* = 86$ . Since in the case of the investi-

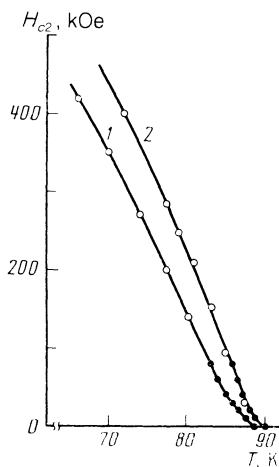


FIG. 12. Temperature dependences of the second critical magnetic field of La-Ba-Cu-O (1) and Y-Ba-Cu-O (2) samples. Here, the measurements in static and pulsed fields are denoted by  $\bullet$  and  $\circ$ , respectively.

gated samples the mean free path was of the order of the coherence length  $\xi$ , we concluded that  $\kappa_1(0) \approx 1.2\kappa$  and  $\kappa_3(0) = 1.3\kappa$ , which gave  $H_{c2}(0) \approx 1.6$  MOe and  $H_{c2}^*(0) \approx 3.1$  MOe, in good agreement with previous estimates.

In view of the possible anisotropy, the value of  $H_{c2}^*(0)$  should be, as demonstrated in Ref. 7, equal to or somewhat less than the maximum critical field  $H_{c2}^{\parallel}(0)$  corresponding to the orientation of the field in the basal plane. Estimates obtained by us for samples with Y demonstrated that the coherence length was

$$\xi^* = [\Phi_0/2\pi H_{c2}^*(0)]^{1/2} \approx 10 \text{ \AA},$$

which in this case was only 2.5–3 times greater than the average distance  $\langle d_c \rangle \approx a \approx 3.5\text{--}4 \text{ \AA}$  between carriers and close to the lattice constant along the  $c$  axis (Table I). This was the reason for the very weak influence of the  $RE^{3+}$  magnetic ions on the superconducting properties of the investigated high-temperature superconductors.

A more detailed analysis of the critical fields could be made, for example, on the basis of Ref. 11 where strongly anisotropic type II superconductors with large values of the Ginzburg-Landau parameter  $\kappa$  were considered. However, bearing in mind the incompleteness and some indeterminacy of the experimental results, we simply concluded that the thermodynamic critical field  $H_c(0)$  was fairly high (15–20 kOe) and the parameter could reach 100. The depth of penetration of the field  $\lambda = \kappa\xi$  was then  $\sim 0.1 \mu\text{m}$ , in agreement with the estimate of  $\lambda$  deduced from the magnetization curves.

#### 4. CURRENT-VOLTAGE CHARACTERISTICS AND TRANSPORT PROPERTIES

In an investigation of the transport properties of high-temperature superconductors it was found in the very first experiments that it was difficult to form good electrical contacts between samples and leads. Even when the contact area was relatively large (1–5 mm<sup>2</sup>), the voltage drop across a contact in the presence of currents up to 0.1 A could be several thousands times greater than the potential difference across a sample. Hence, we concluded that a surface layer with a very low conductivity formed in the region of a contact. If we assume that the thickness of such a layer does not exceed several lattice constants, we find that the resistivity of the layer should be  $10^6\text{--}10^7 \Omega \cdot \text{cm}$ .

The current-voltage characteristics of contacts between high-temperature superconductors and normal metals investigated by us in a wide range of temperatures demonstrated that they were similar to the current-voltage characteristics of tunnel contacts between conventional superconductors and normal metals, particularly when the ohmic component ( $U/I = \text{const}$ ) was subtracted from the recorded dependences  $I(U)$ . The  $\Delta I(U)$  dependences obtained in this way for a tunnel contact between a normal metal and our yttrium sample ( $T_c = 90$  K) are plotted in Fig. 13a for several temperatures. When the temperature of a sample was increased from 4.2 to 92 K, the nonlinearity of the current-voltage characteristic decreased, approaching linearity. Moreover, the current-voltage characteristic was fully symmetric when the applied voltage was reversed.

The current-voltage characteristics obtained in the present study differed from the usual curves by an additional

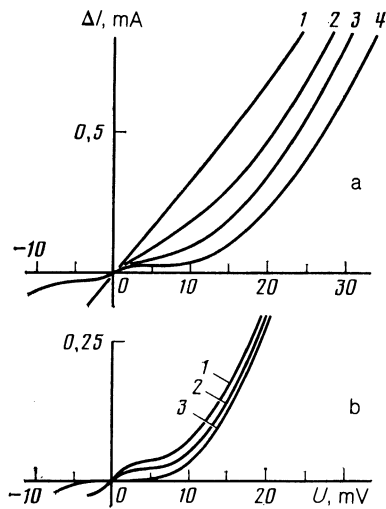


FIG. 13. Current-voltage characteristics of a tunnel contact between a normal metal and a high-temperature yttrium superconductor: a) at various temperatures  $T = 92, 48, 20,$  and  $4.2$  K (curves 1, 2, 3, and 4, respectively); b) at  $T = 4.2$  K in different magnetic fields  $H = 0, 40$  kOe, and  $80$  kOe (curves 1, 2, and 3, respectively).

nonlinearity near the origin of the coordinates, which could be attributed to the presence of a very small gap  $\Delta' \ll k_B T_c$ . This singularity was flattened and vanished when a sufficiently strong magnetic field was applied (Fig. 13b) and the main inflection of the current-voltage characteristic then shifted toward higher voltages.

Estimates of the energy gap  $\Delta(0)$  from the position of the main inflection of the current-voltage characteristics obtained at low temperatures gave approximately the same values of the ratio  $2\Delta(0)/k_B T_c \approx 3.5 \pm 0.3$  for high-temperature superconductors containing yttrium ( $T_c = 90$  K) and for  $\text{La}_{1.8}\text{Sr}_{0.2}\text{CuO}_{4-x}$  ( $T_c \approx 40$  K). However, it should be pointed out that the value of  $\Delta$  deduced from the current-voltage characteristics represented the properties of a material near the surface. In view of the possible deficit of oxygen in the surface layer, the values of  $\Delta$  obtained in this way could differ from those deduced from the bulk characteristics of the superconductor, for example, from the attenuation of ultrasound or from NMR.

Figure 14 shows typical temperature dependences of the resistance obtained for some high-temperature superconductors. The resistance of single-phase samples of  $\text{La}_{1.8}\text{Sr}_{0.2}\text{CuO}_{4-x}$  and  $\text{REBa}_2\text{Cu}_3\text{O}_{7-x}$  with steep superconducting transition temperatures and a low resistivity  $\rho(300 \text{ K}) < 5 \cdot 10^{-3} \Omega \cdot \text{cm}$  increased by a factor of 1.3–3 and almost linearly when temperature was increased from  $1.2T_c$  to 180–220 K. In the range 220–240 K the  $\rho(T)$  dependences had a kink (curves 1 and 2 in Fig. 14), which could be manifested particularly strongly in the case of samples consisting of several phases and characterized by a high resistivity  $\rho(300 \text{ K}) \gg 10^{-3} \Omega \cdot \text{cm}$ . It was interesting to note that anomalies of other properties of high-temperature superconductors could also appear at these temperatures.<sup>12</sup>

The magnetoresistance of high-temperature superconductors was measured in static and pulsed magnetic fields. As in the case of molybdenum chalcogenides,<sup>13</sup> the magnetoresistance was low. For example, in the case of the compound with yttrium it was found that the relative increase in

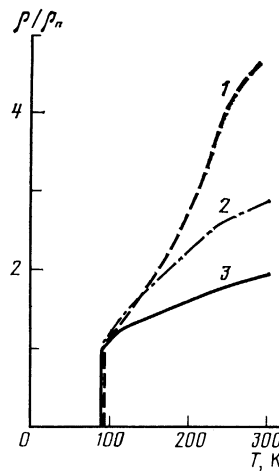


FIG. 14. Temperature dependences of the resistivity of several high-temperature superconductors: 1) Y-Ba-Cu-O,  $\rho(300 \text{ K}) \approx 2 \cdot 10^{-3} \Omega \cdot \text{cm}$ ; 2) Lu-Ba-Cu-O,  $\rho(300 \text{ K}) \approx 3 \cdot 10^{-3} \Omega \cdot \text{cm}$ ; 3) Er-Ba-Cu-O,  $\rho(300 \text{ K}) \approx 1 \cdot 10^{-3} \Omega \cdot \text{cm}$ .

$\rho$  at  $T \approx 1.2T_c$  was 3–5% in a field of 500 kOe.

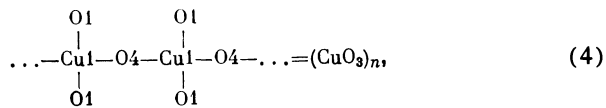
The density of the critical current estimated from the magnetization curves of samples with Y, Lu, and Gd (Fig. 8) was  $(1-2) \times 10^4 \text{ A/cm}^2$  at  $T = 4.2$  K and it decreased by a factor of 10–50 on increase in temperature to 77 K. Other methods for the determination of  $J_c$  (including measurement of the magnetic field frozen in hollow tubes and direct measurements on extended samples) gave results which agreed well with the published values for polycrystalline samples containing yttrium.<sup>14</sup>

## 5. DISCUSSION OF RESULTS

The available data leave no doubt that the superconductivity of the investigated metal oxide compounds is due to the pairing of electrons. However, the actual mechanism of pairing in high-temperature superconductors is not clear. It should be stressed immediately that the various investigations of the properties of high-temperature superconductors have failed to reveal any exotic singularities which would distinguish them (apart from the high values of  $T_c$ ) clearly from other known superconductors. In fact, investigations of high-temperature superconductors in magnetic fields have confirmed that their properties are similar to strongly anisotropic type II superconductors with large values of the Ginzburg–Landau parameter  $\kappa$ . If we bear in mind that the phonon spectrum of high-temperature superconductors may include, because of the small mass of oxygen, Einstein-type modes<sup>15</sup> with fairly high frequencies ( $\omega \gtrsim 2\pi T_c$ ), which should make the greatest contribution to the pairing of electrons,<sup>16</sup> it seems quite proper to consider the properties of these high-temperature superconductors using the traditional BCS phonon mechanism. We shall do this by considering the most important (from our point of view) characteristics of the crystal structure of these superconductors.

Our data definitely indicate that  $T_c$  of the  $\text{REBa}_2\text{Cu}_3\text{O}_{7-x}$  series is practically independent of the atomic number of RE, but is governed by the orthorhombic distortion of the unit cell  $(b-a)/(b+a)$  (Table I, Fig. 1). At the highest values of the distortion the oxygen ions be-

come ordered in the basal plane in such a way that they form chains of the type



oriented along the  $b$  direction,<sup>4</sup> as shown in Fig. 2. The binding of the ions within the chains is due to the overlap of the  $d_{x^2-y^2}$  orbitals of copper at the Cu1 positions and of the  $2p_x$  (or  $2p_y$ ) oxygen orbitals at the O1 (or O4) positions.<sup>17</sup> These chains (which can be regarded as extended one-dimensional clusters) are bound quite weakly to a two-dimensional network of the Cu2, O2, and O3 ions, as can be assessed from the large difference between the distances  $D_{11}(\text{Cu1-O1}) \approx 1.85 \text{ \AA}$  and  $D_{12}(\text{O1-Cu2}) \approx 2.28 \text{ \AA}$ . Estimates of the degree of ionization of copper at the Cu1 and Cu2 positions deduced from the distances  $D_{ij}$  are 2.45 and 2.27, respectively.<sup>4</sup>

In the case of a perfect rigid lattice of  $\text{REBa}_2\text{Cu}_3\text{O}_7$  we find from the calculations of Ref. 17 that the Fermi level  $\varepsilon_F$  is located almost half-way between two  $3d_{x^2-y^2}$  energy bands, which should ensure conduction in an ideal crystal. The states in the  $3d_{x^2-y^2}$  band are vacant, because the bottom is located  $\Delta\varepsilon = \varepsilon_B - \varepsilon_F = 0.11 \text{ eV}$  above  $\varepsilon_F$ . Nevertheless, the calculated density of states  $N(\varepsilon_F)$  should be high and should correspond to  $\gamma_B \sim 25 \text{ mJ} \cdot \text{mol}^{-1} \cdot \text{K}^{-2}$ , which is comparable with  $\gamma \sim 40 \text{ mJ} \cdot \text{mol}^{-1} \cdot \text{K}^{-2}$  deduced from our magnetic susceptibility data.

Since a real crystal has oxygen vacancies (and the maximum values of  $T_c$  are exhibited by  $\text{YBa}_2\text{Cu}_3\text{O}_{7-x}$  samples of nonstoichiometric composition with  $x \approx 0.2$ ), the difference between the energies  $\Delta\varepsilon$  decreases to  $0.06 \text{ eV} \approx 700 \text{ K}$  (Ref. 17).<sup>1)</sup> It also follows from the calculations of Ref. 17 that the small ( $\sim 0.05 \text{ \AA}$ ) displacements of oxygen ions from their equilibrium positions may reduce  $\Delta\varepsilon$  still further. This gives rise to a situation when vibrations of the oxygen ions result in strong mixing of wave functions of the electrons belonging to the  $3d_{x^2-y^2}$  and  $3d_{z^2-y^2}$  bands with considerable fluctuations of the valence state of the copper ions. In other words, this corresponds to the condition of a strong electron-phonon coupling, which may give rise to a high-temperature superconductivity in the case of a sufficiently high stability of the crystal lattice or at least of those structure elements in which the interaction between electrons and phonons is particularly strong. These structure elements in the investigated compounds are the chains of the Cu1 and O4 ions, the stability of which may be ensured by the interaction with two-dimensional networks of the Cu2, O2, and O3 ions. It is interesting to note that the O4 ions in the chains have an anomalously large ( $\sim 0.14 \text{ \AA}$ ), compared with the other positions of oxygen, amplitude of thermal vibrations and the anharmonicity of these vibrations tends to stabilize the crystal structure.<sup>18</sup>

It is therefore very likely that the high density of states and the strong electron-phonon coupling in copper-oxygen chains together with the factors ensuring the structural stability of these chains can give rise to a high-temperature superconductivity in metal oxide compounds.

This model can explain the absence of the usual isotope effect in the case of oxygen in high-temperature supercon-

ductors<sup>19,20</sup> as due to the anharmonicity of the vibrations of the O4 ions because it is these ions that should ensure high values of  $T_c$  in the case of metal oxide systems. In fact, an allowance for the anharmonicity may give rise to a more complex dependence of  $T_c$  on the isotopic mass than that deduced from a simple analysis based on the traditional BCS theory. For example, the anomalous isotope effect in the case of tin has been investigated earlier in a study of the  $\text{SnMo}_6\text{S}_8$  system<sup>21</sup> and it has been found that the vibrations of the Sn ions are also characterized by a large amplitude and anharmonicity; this effect has also been reported for the Pd-H system in which hydrogen is replaced with deuterium and tritium.<sup>22,23</sup> Therefore, the absence of the usual isotope effect should not be regarded as the decisive argument against the phonon mechanism of electron pairing.

The existence of local modes of the Einstein type, due to vibrations of the O4 ions, in the phonon spectrum of a high-temperature superconductor can explain the almost linear rise of the resistivity  $\rho(T)$  between 100 and 240 K (Fig. 14). Simple estimates indicate that these modes can be responsible for the linear rise of  $\rho(T)$  in the range from  $0.2 \Theta_E$  to  $\Theta_E$  ( $k_B \Theta_E = \hbar \omega_E$ , where  $\omega_E$  is the characteristic frequency of the Einstein vibrations). This same explanation has been used earlier<sup>24</sup> to account for the linear dependences  $\rho(T)$  between 15 and 100 K exhibited by several ternary molybdenum sulfides for which  $\Theta_E$  amounts to 50–100 K.

The values  $T_c$  found by us and by other authors<sup>25</sup> and listed in Table I demonstrate that the critical temperature remains practically the same when nonmagnetic yttrium is replaced with rare earths characterized by large localized magnetic moments. This may be a consequence of a short coherence length  $\xi \approx 10 \text{ \AA}$  and predominant localization of Cooper pairs in copper-oxygen chains, which are located relatively far from the  $\text{RE}^{3+}$  ions. The absence of an interaction between the magnetic and superconducting subsystems is supported by the measurements of the magnetic properties of the superconducting state of high-temperature superconductors containing Gd (Figs. 5, 6, and 8). In spite of the apparent difference between the magnetization curves of the samples containing Y and Gd, the data for  $\text{GdBa}_2\text{Cu}_3\text{O}_{7-x}$  can be represented as a sum of the purely superconducting and purely magnetic contributions, and the magnitude of the latter is in good agreement with the results obtained at temperatures  $T > T_c$ .

Our experimental results, namely the correlation between  $T_c$  and the orthorhombic lattice distortion, the weak influence of the magnetic moment of the rare earths on  $T_c$ , the absence of an interaction between the superconducting and magnetic subsystems, the high values of  $H_{c2}(T)$ , and the linear temperature dependence of the resistivity in the range  $T > T_2$  are all evidence of the special role of the  $-\text{O}-\text{Cu1}-\text{O}-$  chains in the formation of the superconducting state in  $\text{REBa}_2\text{Cu}_3\text{O}_{7-x}$  compounds.

Although the available data can be interpreted on the basis of the phonon pairing of electrons, the special features of the structure (weakly bound chains and networks in which the copper ions are in very different valence states) are such that they do not exclude the possibility of the non-phonon pairing mechanisms such as those related to excitons,<sup>26,27</sup> resonant valence bonds,<sup>28</sup> or spin fluctuations.<sup>29,30</sup> The nature of the superconducting state in metal oxide compounds can be identified by further studies of their proper-

ties using samples of higher quality, particularly single crystals.

The authors are grateful to Yu. A. Deniskin and L. N. Bogacheva for their help in the measurements and in the preparation of the samples.

<sup>11</sup>It is interesting to note that cooling below  $T^* = 600\text{--}1000$  K induces a structural transition in  $\text{YBa}_2\text{Cu}_3\text{O}_{7-x}$  from the tetragonal ( $a = b$ ) to the orthorhombic ( $a \neq b$ ) phase and the temperature  $T^*$  of the transition depends on the oxygen content.

<sup>1</sup>J. G. Bednorz and K. A. Müller, *Z. Phys. B* **64**, 189 (1986).

<sup>2</sup>M. K. Wu, J. R. Ashburn, C. J. Torng, P. H. Hor, R. L. Meng, L. Gao, Z. J. Huang, Y. Q. Wang, and C. W. Chu, *Phys. Rev. Lett.* **58**, 908 (1987).

<sup>3</sup>C. W. Chu, P. H. Hor, R. L. Meng, L. Gao, Z. J. Huang, and Y. Q. Wang, *Phys. Rev. Lett.* **58**, 405 (1987).

<sup>4</sup>J. J. Capponi, C. Chaillout, A. W. Hewat, P. Lejay, M. Marezio, N. Nguyen, B. Raveau, J. L. Soubeyroux, J. L. Tholence, and R. Tournier, *Europhysics Lett.* **3**, 1301 (1987).

<sup>5</sup>J. O. Willis, Z. Fisk, J. D. Thompson, S. W. Cheong, R. M. Aikin, J. L. Smith, and E. Zirngiebl, *J. Magn. Magn. Mater.* **67**, L139 (1987).

<sup>6</sup>D. Shoenberg, *Proc. R. Soc. London Ser. A* **175**, 49 (1940).

<sup>7</sup>T. R. Dinger, T. K. Worthington, W. J. Gallagher, and R. L. Sandstrom, *Phys. Rev. Lett.* **58**, 2687 (1987).

<sup>8</sup>N. E. Alekseevskii, A. V. Mitin, C. Bazan, N. M. Dobrovol'skii, and B. Rączka, *Zh. Eksp. Teor. Fiz.* **74**, 384 (1978) [*Sov. Phys. JETP* **47**, 199 (1978)].

<sup>9</sup>N. E. Alekseevskii, C. Bazan, A. V. Mitin, T. Mydlarz, E. P. Kransnoperov, and B. Rączka, *Phys. Status Solidi B* **77**, 451 (1976).

<sup>10</sup>K. Maki, *Physics* (Long Island City, N.Y.) **1**, 127 (1964); P. G. de Gennes, *Phys. Kondens. Mater.* **3**, 79 (1964).

<sup>11</sup>A. V. Balatskii, L. I. Burlachkov, and L. P. Gor'kov, *Zh. Eksp. Teor. Fiz.* **90**, 1478 (1986). [*Sov. Phys. JETP* **63**, 866 (1986)].

<sup>12</sup>J. T. Chen, L. E. Wenger, C. J. McEwan, and E. M. Logothetis, *Phys. Rev. Lett.* **58**, 1972 (1987).

<sup>13</sup>N. E. Alekseevskii, A. V. Mitin, V. N. Samosyuk, and V. I. Firsov, *Zh. Eksp. Teor. Fiz.* **85**, 1092 (1983) [*Sov. Phys. JETP* **58**, 635 (1983)].

<sup>14</sup>R. J. Cava, B. Batlogg, R. B. Van Dover, D. W. Murphy, S. Sunshine, T. Siegrist, J. P. Remeika, E. A. Rietman, S. Zahurak, and G. P. Espinosa, *Phys. Rev. Lett.* **58**, 1676 (1987).

<sup>15</sup>J. M. Tranquada, S. M. Heald, A. Moodenbaugh, and M. Suenaga, *Phys. Rev. B* **35**, 7187 (1987).

<sup>16</sup>G. Bergmann and D. Rainer, *Z. Phys.* **263**, 59 (1973).

<sup>17</sup>M. H. Whangbo, M. Evain, M. A. Beno, and J. M. Williams, *Inorg. Chem.* **26**, 1831, 1832 (1987).

<sup>18</sup>J. B. Goodenough, G. Demazeau, M. Ponchard, and P. Hagenmuller, *J. Solid State Chem.* **8**, 325 (1973).

<sup>19</sup>B. Batlogg, R. J. Cava, A. Jayaraman, R. B. van Dover, G. A. Kourouklis, S. Sunshine, D. W. Murphy, L. W. Rupp, H. S. Chen, A. White, K. Short, A. M. Majsce, and E. A. Rietman, *Phys. Rev. Lett.* **58**, 2333 (1987).

<sup>20</sup>L. C. Bourne, M. F. Crommie, A. Zettl, H. C. zur Loye, S. W. Keller, K. L. Leary, A. M. Stacy, K. J. Chang, M. L. Cohen, and D. E. Morris, *Phys. Rev. Lett.* **58**, 2337 (1987).

<sup>21</sup>N. E. Alekseevskii and V. I. Nizhankovskii, *Zh. Eksp. Teor. Fiz.* **87**, 1877 (1984) [*Sov. Phys. JETP* **60**, 1081 (1984)].

<sup>22</sup>B. Stritzker and W. Buckel, *Z. Phys.* **257**, 1 (1972).

<sup>23</sup>J. E. Schirber, J. M. Mintz, and W. Wall, *Solid State Commun.* **52**, 837 (1984).

<sup>24</sup>N. E. Alekseevskii, A. V. Mitin, E. P. Khlybov, C. Bazan, B. Greñ, and A. Gilewski, *Phys. Status Solidi A* **86**, 398 (1984).

<sup>25</sup>P. H. Hor, R. L. Meng, Y. Q. Wang, L. Gao, Z. J. Huang, J. Bechtold, K. Forster, and C. W. Chu, *Phys. Rev. Lett.* **58**, 1891 (1987).

<sup>26</sup>W. A. Little, *Phys. Rev. A* **134**, 1416 (1964).

<sup>27</sup>V. L. Ginzburg *Phys. Lett.* **13**, 101 (1964).

<sup>28</sup>P. W. Anderson, *Science* **235**, 1196 (1987).

<sup>29</sup>A. V. Vedyaev, O. A. Kotel'nikova, M. Yu. Nikolaev, and A. V. Stefanovich, *Phase Transitions and Electron Structure of Alloys* [in Russian], Moscow State University (1986), Chaps. IX and X.

<sup>30</sup>V. J. Emery, *Phys. Rev. Lett.* **58**, 2794 (1987).

Translated by A. Tybulewicz